ELSEVIER

Journal of Nuclear Materials 290–293 (2001) 805–811

journal of nuclear materials

www.elsevier.nl/locate/jnucmat

Multi-machine modelling of divertor geometry effects

A. Loarte *

European Fusion Development Agreement – Close Support Unit, Max-Planck-Institut für Plasmaphysik, Boltzmannstraße 2, D-85748 Garching, Germany

Abstract

The design and construction of advanced divertors has been one of the main topics of tokamak research during the last decade. The design of such divertors has been carried out by using 2-D plasma edge modelling codes. Many of the predictions from the modelling, which guided the optimisation procedure, have been demonstrated experimentally such as: larger operating density range for partially detached plasmas in vertical divertors compared to horizontal ones, improvement of the divertor pumping capability with more closed divertors and corresponding changes in recycling impurity exhaust following predictions. New phenomena that were hinted at by modelling but not clearly quantified, such as the increase in radiative capability of the divertor induced by the geometry, have been measured and understood by 2-D modelling. Divertor flows determined by divertor sources, which are in turn determined by the geometry, show the expected qualitative trends but detailed modelling which includes plasma drifts, not yet carried out, is required to sort out the effects of drifts and particle sources.

Keywords: Alcator C-Mod; JET; JT-60U; DIII-D; Divertor; 2D model

1. Introduction

During the last decade, one of the key drivers for the design and upgrade of the current generation of tokamaks has been the incorporation of advanced divertors [1–5]. The design of such divertors has been optimised by means of 2-D plasma edge codes, such as B2-Eirene, EDGE2D-NIMBUS and UEDGE [6–11], in order to maximise the benefits that can be expected from successful divertor operation: access to regimes of low divertor power deposition (with high divertor radiation) which are compatible with good bulk plasma performance, reduction of the ionisation source in the main plasma and enhancement of hydrogen pumping leading to good main plasma density control, impurity enrichment in the divertor leading to higher main plasma purity, enhanced helium pumping necessary for reactor tokamaks, etc., which are of paramount importance for the development of a next-step tokamak such as ITER [12].

In order to achieve these objectives, most divertor tokamaks (Alcator C-mod, ASDEX-U, DIII-D, JET, JT-60U, etc.) have modified their divertors and conducted dedicated experimental campaigns to assess whether these predicted beneficial effects of divertor geometry are reproduced in the experiment. This paper reviews the main results obtained in the course of this activity.

2. Modelling of divertor geometry effects on detachment and divertor power load

The initial drive in optimising divertor designs was the need to solve the power load problem in next-step tokamaks [12]. In order to achieve an acceptable peak power load on the divertor of a tokamak such as ITER, it is required that a large proportion of the power flow into the plasma edge (typically ~60%) is lost in the divertor via volumetric processes such as hydrogen and impurity radiation before reaching the divertor target. These losses can only be achieved in a low temperature/high density divertor close to plasma detachment [13,14].

The area of the divertor target which is subject to the largest power fluxes is obviously the separatrix strike

* Tel.: +49-89 3299 4219; fax: +49-89 3299 4312.
E-mail address: loartea@ipp.mpg.de (A. Loarte).

0022-3115/01/$ - see front matter
PII: S0022-3115(00)00456-6

point and, therefore, the divertor designs have been optimised to maximise the volumetric losses near the separatrix. In order to study this problem, 2-D codes have been used to determine the divertor design which favours this effect most and found this to be a vertical divertor [15,16]. In a vertical divertor, the recycling neutrals are emitted towards the separatrix, which becomes a region of preferential ionisation, decreasing the temperature and increasing the density in its vicinity. This concentration of recycling neutrals promotes separatrix detachment at lower main plasma densities and increased volumetric energy and particle (recombination) losses in the separatrix region. On the contrary, a horizontal divertor with outwards inclined target plates concentrates the recycling neutrals away from the separatrix and, therefore, leads to detachment starting away from the separatrix rather than close to it, as is required for optimum divertor operation. Such a difference in divertor behaviour was predicted with B2-Eirene for the JET-Mk IIA divertor [17] and found experimentally [18]. Figs. 1(a) and (b) show the predicted recombination strengths for two similar B2-Eirene runs displaying the behaviour described above: plasma recombination close to the separatrix for vertical divertor discharges and away from the separatrix for horizontal divertor discharges. Fig. 1(c). shows the inner divertor experimental detachment behaviour, characterised by the degree of detachment (DoD), where $\mathrm{DoD} > 1$ implies divertor detachment [19], for two comparable density scans on the JET-Mk IIA horizontal and vertical target. While the vertical divertor shows detachment starting at the separatrix and progressing smoothly across the SOL with increasing density, the horizontal divertor shows the plasma detaching away from the separatrix, with the separatrix plasma itself remaining attached until the formation of a divertor MARFE. Observations displaying similar effects have been reported from Alcator C-mod [20] and ASDEX-U [21].

One of the problems in the achievement of a detached divertor plasma is the asymmetry between inner and outer divertors (related to plasma drifts and geometry effects) and which, for the normal direction of the toroidal field, makes the inner divertor reach detachment at lower densities than the outer one. Physically separating the inner and outer divertors and feeding the gas separately to either divertor was expected to allow some control of the detachment asymmetry in JET-Mk II Gas Box. Such behaviour has indeed been found experimentally in agreement with the predictions from EDGE2D-NIMBUS [22]. Changing the location of the gas puff from the inner to the outer divertor makes detachment occur almost at the same density for both divertors. When gas is puffed at the inner divertor, the density limit is reached with a totally detached inner divertor and a fully attached outer divertor [22].

The achievement of separatrix detachment at lower densities for a vertical divertor does not necessarily lead to a lower L-mode density limit. The L-mode density limit is very well correlated with the onset of total ion recombination at the divertor [23], which is much less sensitive to the geometry of the divertor target [21]. Modelling for ASDEX-U Div I and Div II (shown in Fig. 2) demonstrates that the range of densities in which separatrix detachment is obtained is much larger in Div II than in Div I, but this does not imply a smaller range of operating densities in terms of total divertor detachment, as shown by the drop of the integrated ion flux.

Besides allowing an easier access to separatrix detachment, a vertical divertor creates an extended region of low electron temperature in the vicinity of the separatrix [21]. This temperature profile favours the formation of large radiating volumes so that the amount of divertor radiation can be a large proportion of the power flowing into the divertor, as required for next-step devices [12]. Such extended radiation pattern has been measured in ASDEX-U and is in very good agreement with B2-Eirene modelling (see Fig. 3). Recent studies on the nature and size of this carbon radiation in ASDEX-U [24] have demonstrated that the divertor geometry leads to these large radiated powers in the following way: the divertor geometry of Div II leads to the formation of an extended region around the separatrix with high electron density and low divertor temperature at lower separatrix density in Div II than in Div I. The amount of divertor radiation is then determined by the electron temperature at the divertor and the size of the carbon source (i.e., chemical sputtering yield). For typical ASDEX-U conditions, the proportion of power reaching the divertor is typically less than 40% of the edge power flow, when the divertor temperature is few eV, which is in agreement with the experimental measurements [24].

A further obvious effect of the divertor geometry on the power flux is to allow the diffusion of energy into the private flux region by anomalous plasma transport. This effect has been studied in DIII-D by scanning the X-point to wall distance and found to cause a drop of about a factor of 2 in the measured peak parallel power flux, when moving the X-point to $\sim$35 cm from the divertor target [25]. Such an effect is sizeable in ASDEX-U as well and can account for a reduction of a factor $\sim$2 in the peak parallel power flux for similar attached discharges in Div I and Div II [21].

3. Modelling of divertor geometry effects on neutral pumping

One of the other main goals of an optimised divertor is to provide good neutral pumping. This is required to obtain good density control in existing experiments, as

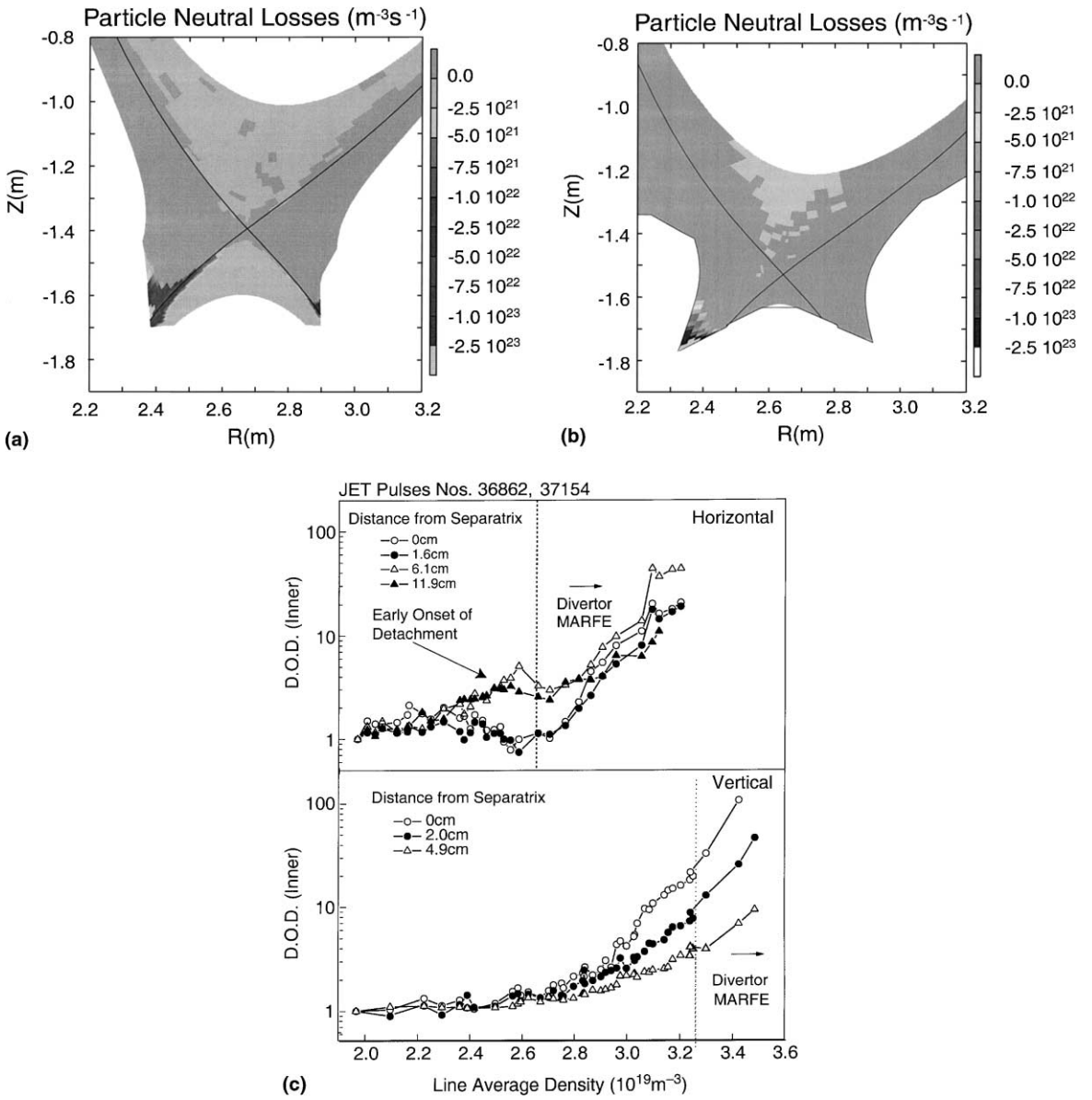

Fig. 1. (a) B2-Eirene divertor particles losses (recombination) for typical L-mode conditions in a vertical divertor JET-Mk IIA discharge [17]. (b) B2-Eirene divertor particles losses (recombination) for typical L-mode conditions in a horizontal divertor JET-Mk IIA discharge [17]. (c) DoD for the inner divertor plasma at various distances from the separatrix for two JET-Mk IIA density scans. The upper figure shows the early onset of detachment for the plasma starting away from the separatrix for horizontal divertor discharges. The lower figure shows detachment starting progressively from the separatrix outwards in the SOL for vertical divertor discharges [18].

well as to remove the helium ash in next-step devices. Increasing the physical divertor closure reduces the escape probability of recycled neutral atoms/molecules reaching the bulk plasma and, therefore, increases the divertor neutral pressure and pumping, as has been measured in JET [26]. Beyond this obvious effect, other effects of divertor geometry on pumping have been determined since the first pumping experiments carried out in DIII-D [27]. The probability of a recycled neutral to be pumped depends on the probability of the neutral reaching the pumping plenum compared to that of being ionised in the plasma. The initial results from DIII-D had shown a very strong dependence of divertor pumping on the geometry itself (in particular, the distance between the strike point and the entrance of the pumping plenum [27]). On the contrary, other

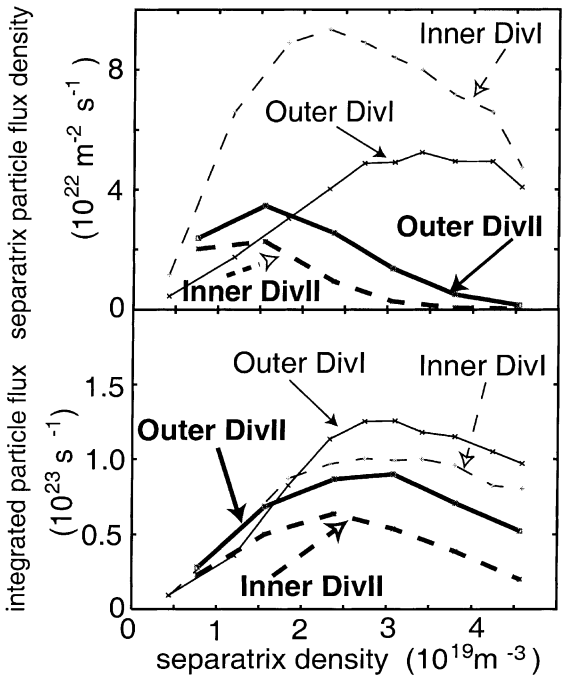

Fig. 2. Inner and outer divertor ion flux (separatrix and integrated) for two density scans in ASDEX-U modelled with B2-Eirene for Div I (horizontal) and Div II (vertical). The upper figure shows the reduction in density required to achieve separatrix detachment in Div II compared to Div I. The lower figure shows the integrated ion flux to inner and outer divertor both for Div I and Div II displaying much smaller differences with respect to total detachment [21].

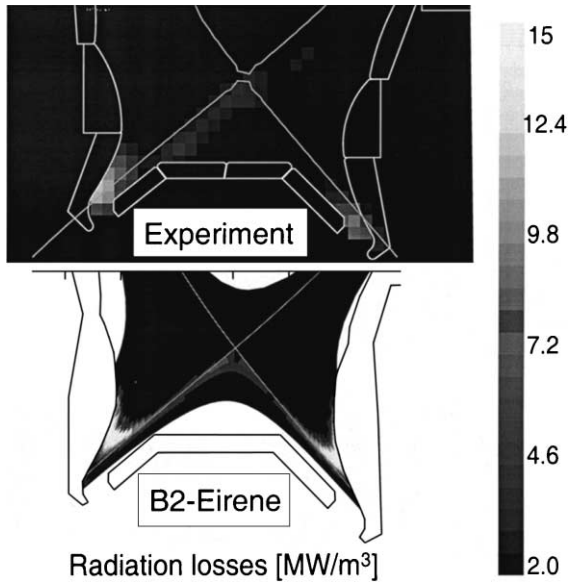

Fig. 3. Measured and B2-Eirene modelled radiation profiles in ASDEX-U Div II showing the extended region of radiation close to the separatrix. The absence of this feature in the measurements for the outer divertor is due to the lack of bolometer channels in this area [21].

experiments have not found such dependence for deuterium pumping but a much smoother one [28,29]. The reason for such a difference was identified in [30] by means of 2-D modelling with EDGE2D-NIMBUS for DIII-D, JET and Alcator C-mod and analytical models. In [30], it was found that divertor pumping depends strongly on the exact position of the plasma with respect to the pumping plenum when the transport of neutrals to the plenum is dominated by a first flight neutral contribution. Otherwise, when the neutral transport to the plenum is dominated by multiple scattering (charge-exchange and multiple collisions with vessel walls), the transport process is diffusive and presents a naturally weaker dependence on the neutral source location. Figs. 4(a) and (b) show a comparison between modelling results from EDGE2D-NIMBUS and experimental measurements from DIII-D and JET-Mk IIA discharges illustrating this point.

These physical neutral transport mechanisms apply not only to deuterium neutrals but also to recycling impurities. In this case, the ballistic component of neutral transport is particularly important, as the recycling impurity neutrals are not subject to charge-exchange in the experiment (due to their low concentrations). Modelling with B2-Eirene for ASDEX-U had predicted that in going from Div I to Div II, the relative pumping of He and Ne would change considerably [21]. In Div I, He and Ne were pumped from the outer side of the SOL and this meant that the atoms with shorter mean free path (Ne) were better confined near the pumping plenum entrance in the divertor. He, which has a longer mean free path, could escape from the divertor more easily and, therefore, its compression in the pumping plenum was low. In the present Div II, pumping takes place through the gaps between the lower parts of the vertical target and the private flux region dome. In this case, the longer mean free path of He facilitates its enrichment in the pumping plenum. Such predictions have been confirmed experimentally, as seen in Fig. 5, which shows the He and Ne decay rates in ASDEX-U Div I and Div II pumping experiments [31]. Similarly, JET-Mk II experiments show preferential He enrichment when the divertor strike point is located near the pumping plenum entrance, for which the probability of neutral He atoms reaching ballisticaly the plenum is highest [30,32].

4. Modelling of divertor geometry effects on plasma flows

As it has already been shown, the divertor geometry has a deep influence on the neutral sources in the divertor plasma and, as a consequence, on divertor plasma

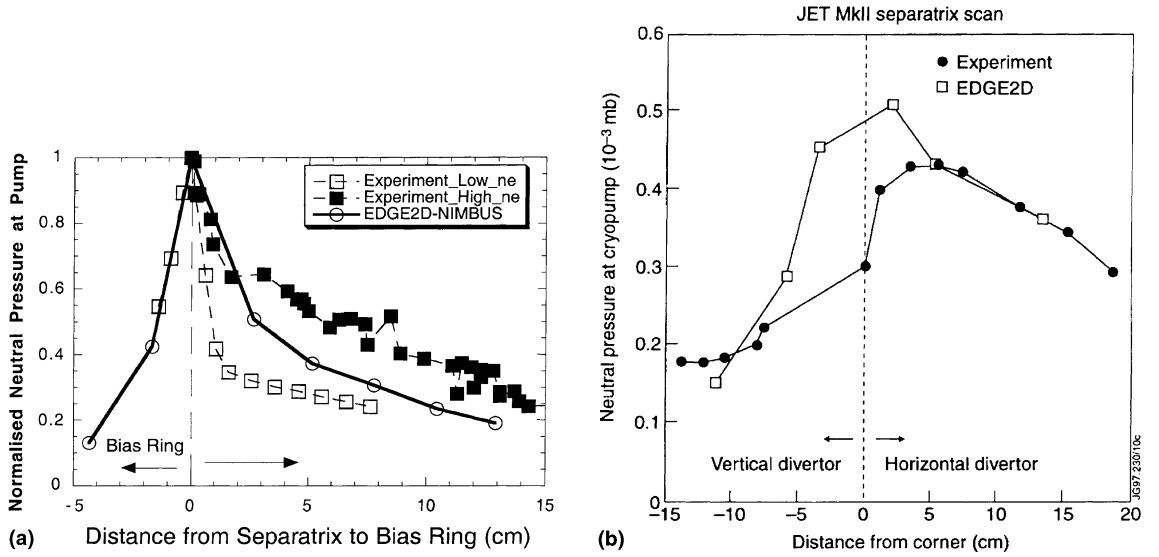

Fig. 4. (a) Experimental and EDGE2D-NIMBUS modelled normalised neutral pressure at the pumping plenum for DIII-D, versus distance from the strike point to the plenum entrance (Bias Ring). The experimental data corresponds to high density and low density ELMy H-mode conditions, while the modelling corresponds to an intermediate density point [30]. (b) Experimental and EDGE2D-NIMBUS modelled neutral pressure at the cryopump for JET-Mk IIA experiments, versus distance from the strike point to the plenum entrance (vertical dashed line) [30].

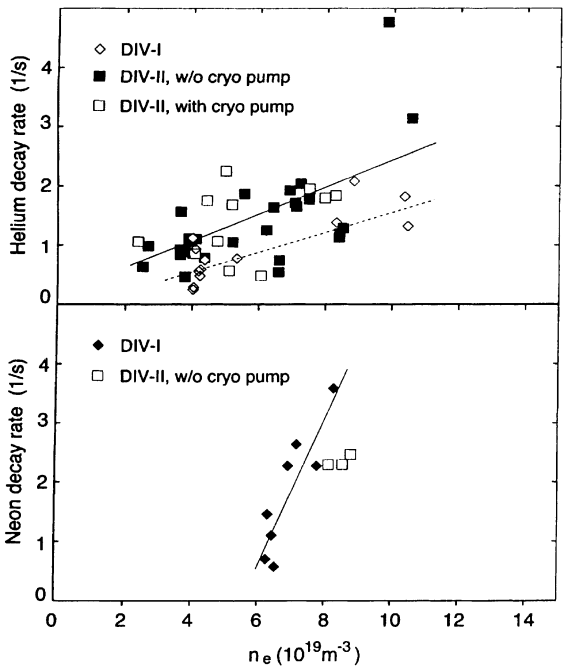

Fig. 5. Experimental decay rates of He and Ne for pumping experiments in ASDEX-U with both divertor configurations Div I (horizontal) and Div II (vertical) showing the improvement in He pumping and the deterioration of Ne pumping in going from Div I to Div II, in agreement with modelling predictions [31].

flows. A major difficulty, when carrying out modelling of these flows, is the need to include plasma flows not driven by particle sources such as drifts. Presently, new versions of 2-D codes are becoming available which include a proper treatment of the classical drift terms (a thorough experimental description of divertor and SOL flows can be found in [33] and their modelling in [34]) and the complete picture of the relative importance of the source-driven and drift flows, both in the SOL and the divertor, remains to be evaluated. Despite this, considerable advances in the measurements, understanding and modelling of 2-D plasma and impurity flows in the divertor have taken place in the last few years [33–39].

The concentration of neutrals towards the separatrix, typical of vertical divertors, tends to create a region of deuterium flow reversal in this area [40]. As a consequence, momentum transport in the divertor region is modified, leading to an inwards diffusion of momentum (through particle diffusion and perpendicular viscosity) [13,41] which, in turn, produces a region of overpressure at the divertor target (compared to the one expected from momentum conservation along the flux tubes and acceleration to Mach 1 at the sheath). Such divertor separatrix overpressure has been observed experimentally in Alcator C-mod and given the name of 'Death Ray' [40].

Reversal of the deuterium flow is not as drastic, in terms of core impurity contamination, as originally feared [13]. This is due to the fact that impurity flow

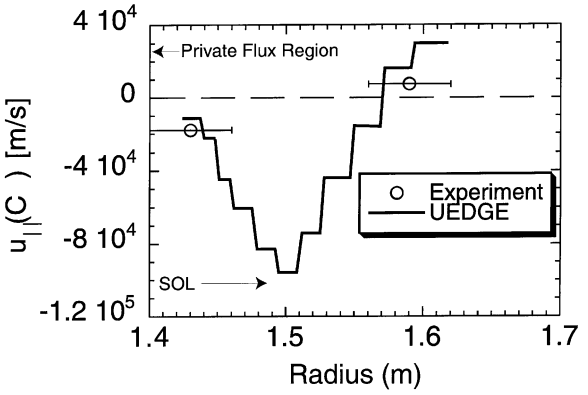

Fig. 6. Experimental and UEDGE modelled velocity of the carbon impurity flows across the SOL versus radial coordinate along the divertor floor. A region of reversed flow close to the separatrix ($u_{\parallel}(C) < 0$) is clearly seen both in code and simulations [39].

reversal is seen to appear even before deuterium flow reversal takes place. Reversal of impurity and deuterium flows have been observed in horizontal divertors, such as DIII-D, as well. Impurity flow reversal in DIII-D occurs at low/medium densities well before deuterium flow reversal is observed [37–39]. The region of impurity flow reversal is concentrated close to the separatrix where the thermal force, which transports impurities against temperature gradients, is largest. Measurements and UEDGE modelling of this impurity flow reversal are in good agreement, as shown in Fig. 6. Deuterium flow reversal in DIII-D occurs at higher densities for attached plasmas near the separatrix, which is in good agreement with UEDGE predictions [39]. When partial detachment starts, the region of deuterium flow reversal disappears as the ionisation front (where $M \sim 1$) moves away from the target. Positive results of the comparison between the measured and B2-Eirene modelled impurity and deuterium flows have also been reported for ASDEX-U [35,36].

5. Conclusions

In this paper, we have summarised the comparisons among the predicted divertor geometry effects and those seen in the experiments. Many of the expected predictions for the detachment behaviour with divertor geometry have been reproduced in the experiment, following quite closely the modelling predictions. In particular, the lower density required to access separatrix detachment for vertical divertor configurations compared to horizontal ones is universally seen. Modelling for ASDEX-U has shown that the low temperature region close to the separatrix, together with the fact that carbon is produced by chemical sputtering, is what allows the divertor radiation to increase when going from Divertor I (horizontal) to Divertor II (vertical).

Another area where there has been a successful experimental confirmation of the divertor geometry effects is divertor pumping. The differences seen among the experiments in the behaviour of the pumped particle flux (for recycling impurities and deuterium neutrals) is well described by the models. Deuterium transport to the pumping plenum can be either diffusive (dominated by wall and charge-exchange collisions), such as in JET-Mk II A, or ballistic (such as in DIII-D) which depends strongly on the divertor and magnetic geometry. In the second case, the exact position of the plasma strike point with respect to the pumping plenum determines the pumped flux, while in the second case, the dependence is weaker. Recycling impurities, such as noble gases, are not subject to charge-exchange and, therefore, their transport tends to be strongly influenced by the geometry of the divertor. This has been clearly shown in changing from Div I to Div II in ASDEX-U, which has lead to a worsening of the Ne compression and an increase of the He compression, as expected from modelling. Similar experiments in the JET-MkII divertor show a clear preferential enrichment when the strike point is located at a position such that the solid angle for helium reaching the pumping plenum is highest.

Divertor plasma flows for impurities and deuterium ions are presently areas of intense research. Although a quantitative comparison of simulations that reproduce experimental plasma flows (which include drifts) has not yet been performed, the predicted effects of divertor geometry on divertor-induced flows have been seen in the experiment. These effects include the occurrence of impurity flow reversal with forward deuterium flow at low densities, seen in DIII-D, and the occurrence of deuterium flow reversal at high densities. Momentum transport across the SOL, associated with these patterns of reversed flows, can cause the formation of regions in which the divertor pressure can exceed the values expected from pressure balance with the upstream SOL profiles. Such phenomena has been studied with models and seen experimentally in Alcator-C-mod (Death Rays). Similarly, the slowing down of the deuterium flow in the recombination region, which is a fundamental physics mechanism to achieve plasma detachment, has been measured in several experiments such as JT-60U [33] and ASDEX-U [35].

Areas where further work is needed to make the comparison between modelling and experiment more quantitative are those associated with SOL flows (thought to be drift-driven) and understanding anomalous transport processes in the SOL, as well as, the role of main chamber recycling in the global particle and energy balance out of the main plasma.

Acknowledgements

This review has been made possible with the help and contributions of those working in the area of divertor research. The author is particularly grateful to the following persons for their contributions, encouragement and helpful comments: N. Asakura, K. Borrass, D.Coster, J. Gafert, M. Groth, L. Horton, A. Kukushkin, B. La Bombard, B. Lipschultz, C. Maggi, G. Matthews, R. Monk, R. Pitts, G. Porter, R. Schneider and D. Stotler.

References

[1] L. Horton et al., Nucl. Fus. 39 (1999) 1.
[2] E. Marmar et al., in: Proceedings of the 17th International Conference on Fusion Energy, Yokohama, 1998, vol. 1, IAEA Vienna, 1999, p. 71.
[3] O. Gruber et al., in: Proceedings of the 17th International Conference on Fusion Energy, Yokohama, 1998, vol. 1, IAEA Vienna, 1999, p. 213.
[4] T. Taylor, DIII-D Team, in: Proceedings of the 17th International Conference on Fusion Energy, Yokohama, 1998, vol. 1, IAEA Vienna, 1999, p. 49.
[5] S. Ishida, JT-60U Team, in: Proceedings of the 17th International Conference on Fusion Energy, Yokohama, 1998, vol. 1, IAEA Vienna, 1999, p. 13.
[6] B.J. Braams, PhD thesis, University of Utrecht, 1986.
[7] D. Reiter et al., Plasma Phys. Control Fus. 33 (1991) 1579.
[8] R. Simonini et al., J. Nucl. Mater. 196–198 (1992) 369.
[9] R. Simonini et al., Contrib. Plasma Phys. 34 (1994) 368.
[10] T.D. Rognlien et al., J. Nucl. Mater. 196–198 (1992) 347.
[11] T.D. Rognlien, Contrib. Plasma Phys. 36 (1996) 105.
[12] R. Parker et al., J. Nucl. Mater. 241–243 (1997) 1.
[13] A.J. Loarte, Nucl. Mater. 241–243 (1997) 118.
[14] A. Kukushkin et al., in: Proceedings of the 17th International Conference on Fusion Energy, Yokohama, 1998, vol. 3, IAEA Vienna, 1999 p. 1013; these Poceedings.
[15] JET Team (presented by G. Vlases), in: Proceedings of the 16th International Conference on Fusion Energy, Montreal, 1996, vol. 1, IAEA Vienna, 1997, p. 371.
[16] R. Schneider et al., J. Nucl. Mater. 241–243 (1997) 701.
[17] K. Borrass et al., in: Proceedings of the 24th European Conference on Controlled Fusion and Plasma Physics, Berchtesgaden, vol. 21A, Part IV, European Physical Society, Geneva, 1997, p. 1461.
[18] R. Monk et al., in: Proceedings of the 24th European Conference on Controlled Fusion and Plasma Physics, Berchtesgaden, vol. 21A, Part I, European Physical Society, Geneva, 1997, p. 117.
[19] A. Loarte et al., Nucl. Fus. 38 (1998) 331.
[20] B. Lipschultz et al., J. Nucl. Mater. 241–243 (1997) 771.
[21] R. Schneider et al., J. Nucl. Mater. 266–269 (1999) 175.
[22] C. Maggi et al., in: Proceedings of the 26th European Conference on Controlled Fusion and Plasma Physics, Maastricht, vol. 23J, European Physical Society, Geneva, 1999, p. 201.
[23] D. Coster et al., J. Nucl. Mater. 266–269 (1999) 804.
[24] D. Coster et al., in: Proceedings of the 26th European Conference on Controlled Fusion and Plasma Physics, Maastricht, vol. 23J, European Physical Society, Geneva, 1999, p. 1571.
[25] C. Lasnier et al., Nucl. Fus. 38 (1998) 1225.
[26] JET Team (prepared by R. Monk) Nucl. Fus. 39 (1999) 1751.
[27] C.C. Keppler et al., Nucl. Fus. 33 (1993) 533.
[28] Saibene et al., in: Proceedings of the 21th European Conference on Controlled Fusion and Plasma Physics, Bournemouth, vol. 19C, Part II, European Physical Society, Geneva, 1995, p. 121.
[29] A. Niemczewski et al., Nucl. Fus. 37 (1997) 151.
[30] A. Loarte et al., in: Proceedings of the 24th European Conference on Controlled Fusion and Plasma Physics, Berchtesgaden, vol. 21A, Part III, European Physical Society, Geneva, 1997, p. 1049.
[31] H.-S. Bosch et al., in: Proceedings of the Fourth International IEA Workshop on Helium Transport and Exhaust in Fusion Devices, 1999, p. 147.
[32] M. Groth et al., in: Proceedings of the Fourth International IEA Workshop on Helium Transport and Exhaust in Fusion Devices, 1999, p. 409.
[33] N. Asakura et al., these Proceedings.
[34] A. Chankin et al., these Proceedings.
[35] J. Gafert et al., J. Nucl. Mater. 266–269 (1999) 365.
[36] D. Coster et al., Czech. J. Phys. 48/S2 (1998) 327.
[37] R. Isler et al., Phys. Plasmas 6 (1999) 541.
[38] J. Boedo, Plasma Physics Division Meeting 1999, American Physical Society, Seattle, USA.
[39] G. Porter et al., in: Proceedings of the 25th European Conference on Controlled Fusion and Plasma Physics, Prague, vol. 22C, European Physical Society, Geneva, 1998, p. 1994.
[40] B. La Bombard et al., J. Nucl. Mater. 241–243 (1997) 149.
[41] D. Stotler et al., J. Nucl. Mater. 266–269 (1999) 947.